Supporting Information

Photocatalytic detoxification of a sulfur mustard simulant by donor-enhanced porphyrin-based Covalent-Organic Frameworks

Yana Chen[a,d], Zewen Shen[a], Yezi Hu[a], Haotian Zhang[a], Lisha Yin[b], Guixia Zhao*[a], Guangtong Hai*[c] and Xiubing Huang*[d]

[a] College of Environmental Science and Engineering, North China Electric Power University, Beijing 102206, P. R. China

[b] Institute of Advanced Materials (IAM), School of Flexible Electronics (Future Technologies), Nanjing Tech University (Nanjing Tech), Nanjing, 211816, P. R. China

[c] Institute of Zhejiang University-Quzhou, Zhejiang University, Quzhou 324000, China

[d] Beijing Advanced Innovation Center for Materials Genome Engineering, Beijing Key Laboratory of Function Materials for Molecule & Structure Construction, School of Materials Science and Engineering, University of Science and Technology Beijing, Beijing 100083, P. R. China

*Corresponding authors

E-mail address: guixiazhao@ncepu.edu.cn (G. Zhao), haigt@zju.edu.cn (G. Hai), xiubinghuang@ustb.edu.cn (X. Huang)

1. General information

All reagents were purchased from commercial suppliers and used without further purification unless stated otherwise. 5,10,15,20-tet-rakis-(4-aminophenyl)-porphyrin (TPH, 98%), 2,5-dihydroxyterephthalaldehyde (DHA, 98%) and 2, 5 -dimethoxyterephthalaldehyde (DMA, 98 %) were purchased from Jilin Chinese Academy of Sciences-Yanshen Technology Co., Ltd. Terephthaldehyde (DA, 97 %), mesitylene (98 %), 1,4-Dioxane (99.5 %), acetic acid (AcOH, ≥ 99.8 %), ethanol absolute (99.5 %, Water ≤ 300 ppm), methanol (99.9%, GC), dimethyl sulfoxide (DMSO, 99.8%), acetonitrile (99.9%), isopropanol (99.9%), 2-Chloroethyl ethyl sulfide (≥ 97%), 1-Chloro-2-(ethylsulfinyl) ethane (≥ 97%) and Tetrahydrofuran (THF, 99 %, AR) were all provided by Aladdin.

1.1 Characterizations

Powder X-ray diffraction (PXRD) analyses were performed using a Rigaku SmartLab SE X-ray diffractometer equipped with a Cu Kα source. Small angle X-ray scattering data collected on a Bruker D8 Advance diffractometer was used to correct the deviation with a step size of 0.01°. Fourier transform infrared spectra (FT-IR) were recorded on a SHIMADZU IRTracer-100. BET surface areas were obtained from N_2 adsorption/desorption isotherms collected at 77 K using Micromeritics TriStar II. Scanning electron microscopy (SEM) images were recorded on a Hitachi SU 8100 Scanning Electron Microscope. Solid-state 13C CP/MAS NMR spectra were collected on a BRUKER AVANCE NEO 400WB spectrometer. X-ray photoelectron spectroscopy (XPS) analyses were performed using a Thermo Scientific ESCALAB 250Xi spectrometer, equipped with a monochromatic Al Kα X-ray source (1486.8 eV). Photoelectrochemical experiments measurements were performed on an electrochemical workstation (CHI760E, CHI Instruments, Shanghai, China). Electron paramagnetic resonance (EPR) spectra were recorded at 293 K with a Bruker EMXnano259 spectrometer, operated at 9.62 GHz with 12.59 mW power and modulation at 100 kHz/1 G. By using $BaSO_4$ as a reflectance standard, the UV–vis DRS of COFs was estimated from 300 to 800 nm by an UV-3600 UV-vis spectrophotometer (Shimadzu, Japan) configured with a diffuse reflectance measurement accessory. Thermogravimetric analysis (TGA) spectra were recorded using a TG/DTA 8122 thermogravimeter under an N_2 atmosphere, with a heating rate of 10 °C min^{-1} from 30 °C to 800 °C. Photoluminescence (PL) spectra were collected on steady-state fluorescence spectrometer (Horiba Fluoromax-4 spectrophotometer). The conversion, selectivity of CEES was monitored by using a Shimadzu GC–MS (GCMS-QP2020 NX) instrument equipped with a Dielectric barrier discharge plasma detector and

a Zebron ZB-Wax column.

1.2 Electrochemical measurements

The Mott-Schottky plots, photocurrent response and electrochemical impedance of the photo-catalysts were measured on an electrochemical workstation (CHI760E, CHI Instruments, Shanghai, China). A white LED (PLS-LED 100C, PerfectLight) was utilized as the light source and 0.5 M Na_2SO_4 aqueous solution was used as the supporting electrolyte throughout the photocurrent measurements. A platinum wire and Ag/AgCl electrode were used as counter electrode and reference electrode, respectively. To prepare the working electrode, 50 μL naphthol together with 1 mL ethanol was mixed with 2 mg catalyst. 50 μL of the mixture was then dipped into ITO, followed by drying in air. Photocurrent measurements were conducted with light on–off cycles and a scan rate of 100 mV s^{-1}. Mott–Schottky measurements were performed under dark conditions at frequencies of 500 Hz, 1000Hz and 1500 Hz. Furthermore, electrochemical impedance spectroscopy (EIS) was conducted under light irradiation at a bias potential of +0.5 V. The potential vs NHE was calculated by using the following Eq:

$$E_{NHE} = E_{Ag/AgCl} + 0.197$$

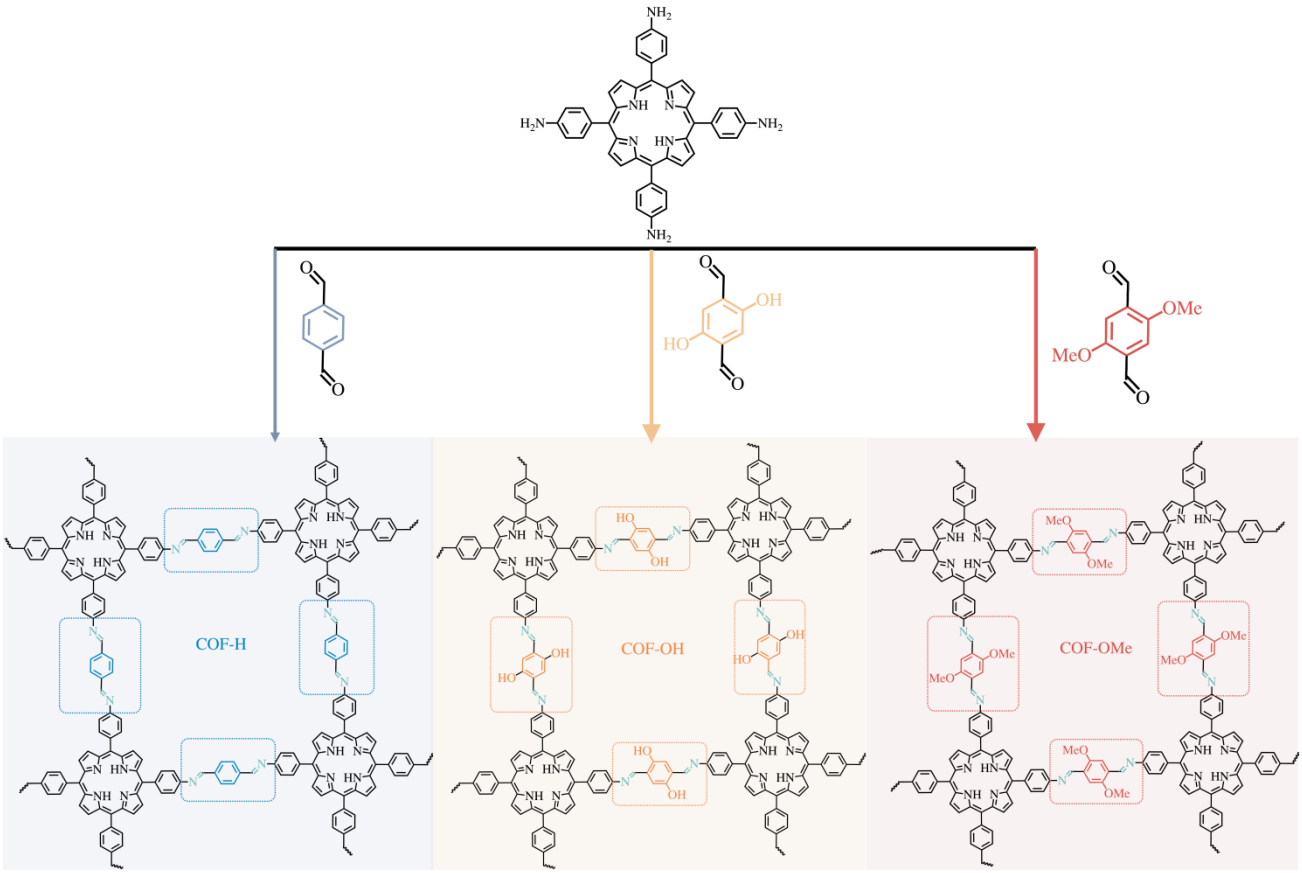

Fig. S1. The schematic diagram for synthesis and structures of COF-H, COF-OH and COF-OMe.

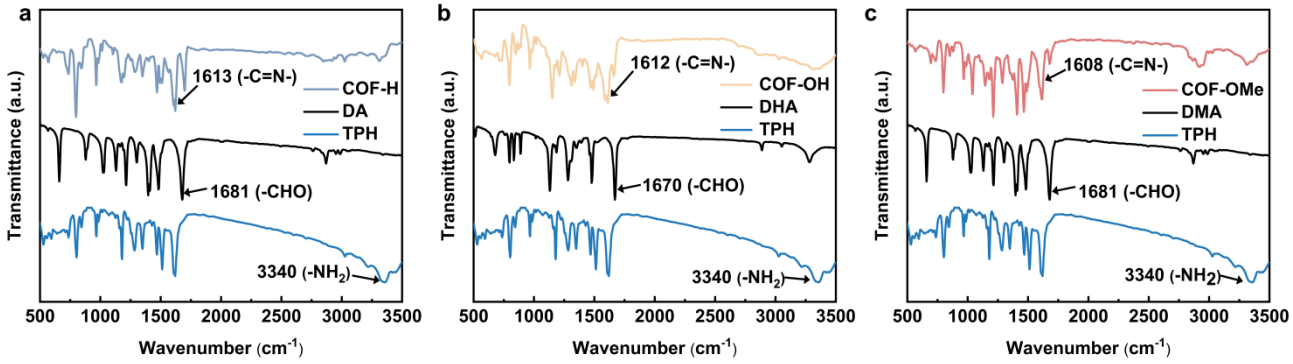

Fig. S2. Fourier transform infrared spectra (FT-IR) of (a) COF-H, (b) COF-OH and (c) COF-OMe.

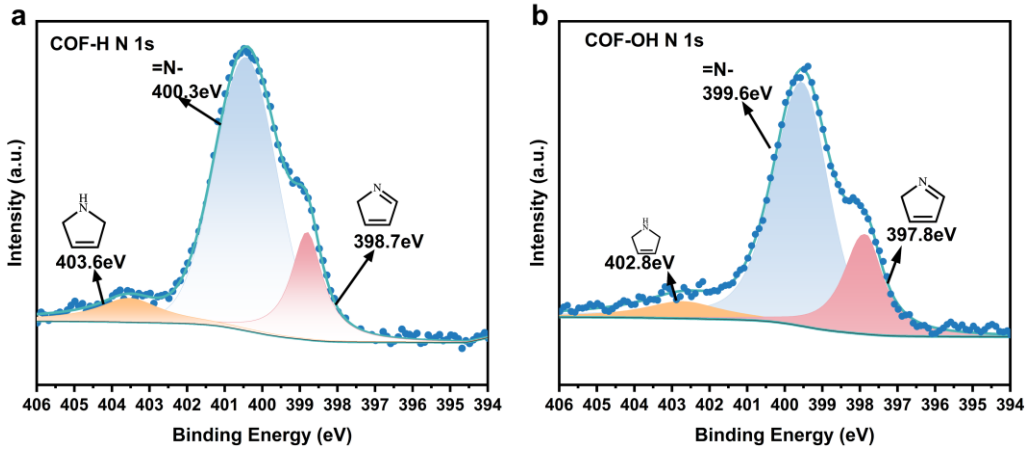

Fig. S3. N 1s XPS spectra of (a) COF-H and (b) COF-OH.

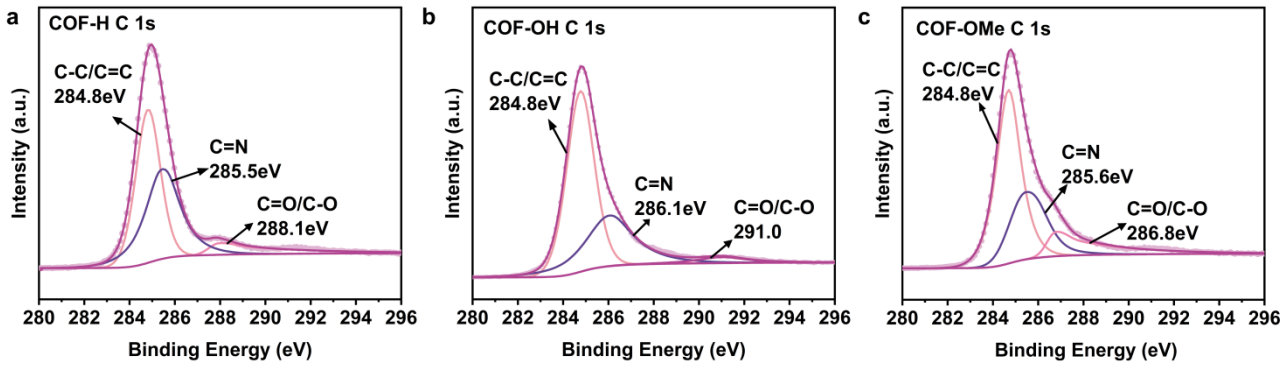

Fig. S4. C 1s XPS spectra of (a) COF-H, (b) COF-OH and (c) COF-OMe.

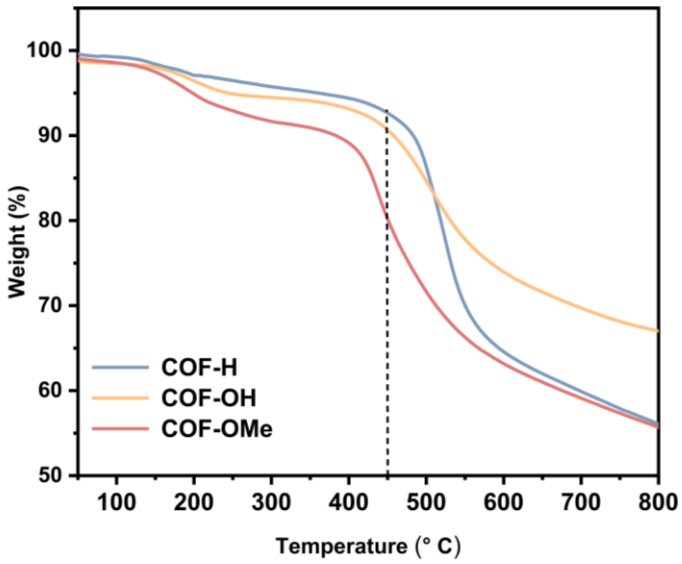

Fig. S5. Thermal gravimetric analysis spectrum of COF-H, COF-OH and COF-OMe.

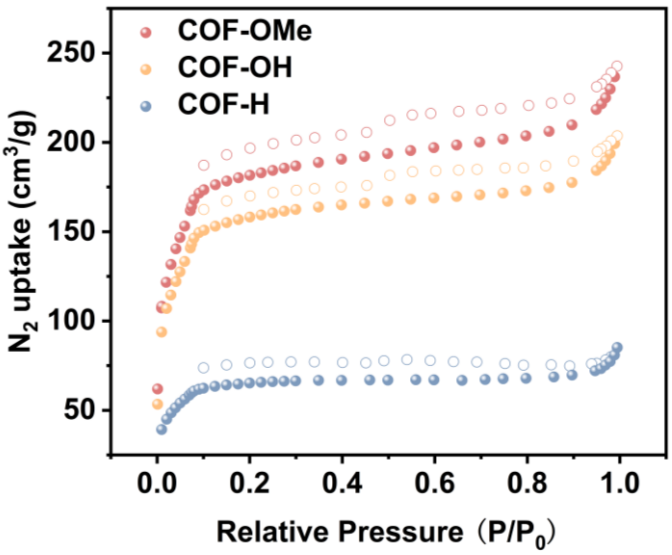

Fig. S6. N_2 sorption isotherms of COF-H, COF-OH and COF-OMe.

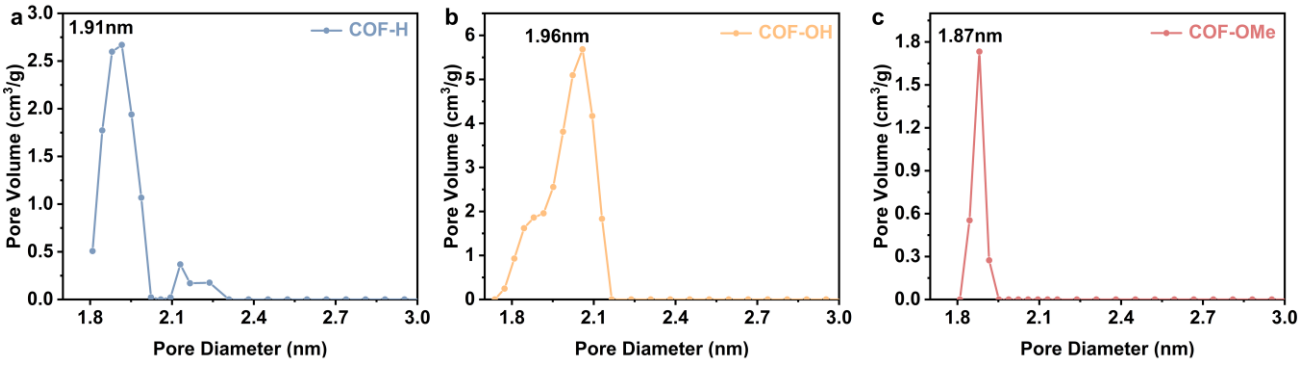

Fig. S7. Pore size distribution of (a) COF-H, (b) COF-OH and (c) COF-OMe.

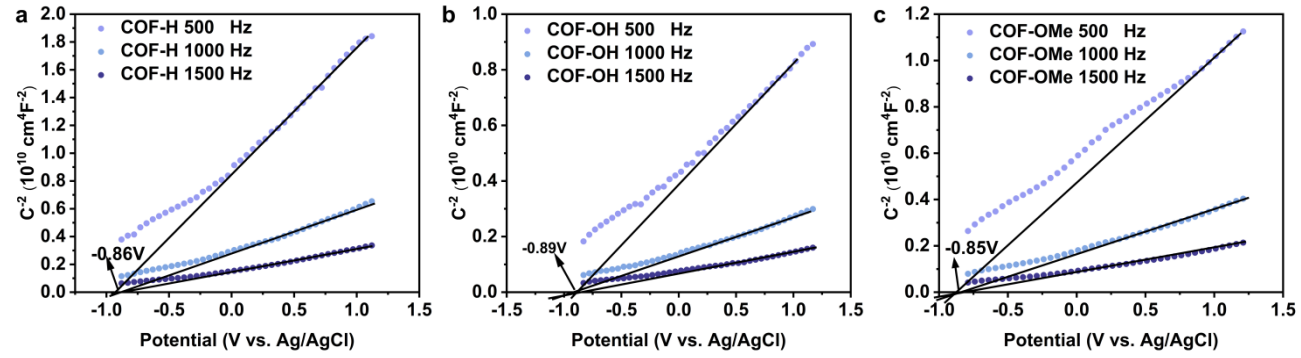

Fig. S8. Mott–Schottky plots of (a) COF-H, (b) COF-OH and (c) COF-OMe at 500 Hz, 1000 Hz and 1500 Hz.

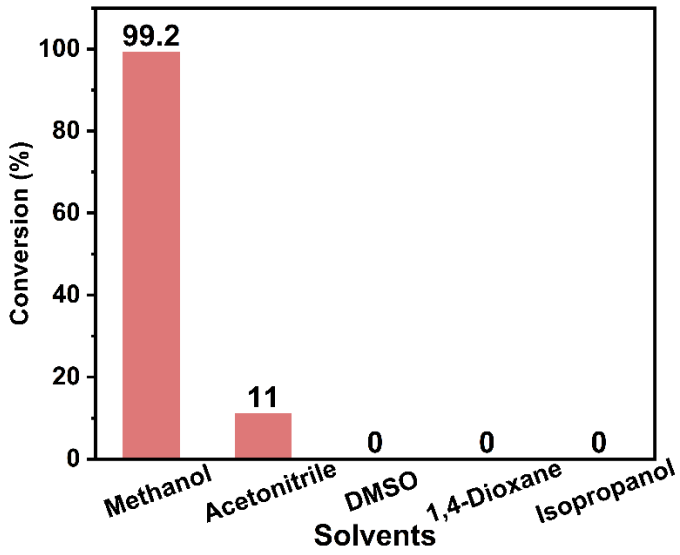

Fig. S9. COF-OMe photocatalyst for selective photocatalytic detoxification of CEES in different solvents. Standard conditions: COFs (5 mg), solvents (5 mL), CEES (0.2 mmol), air, white LED. Reaction time: 3h.

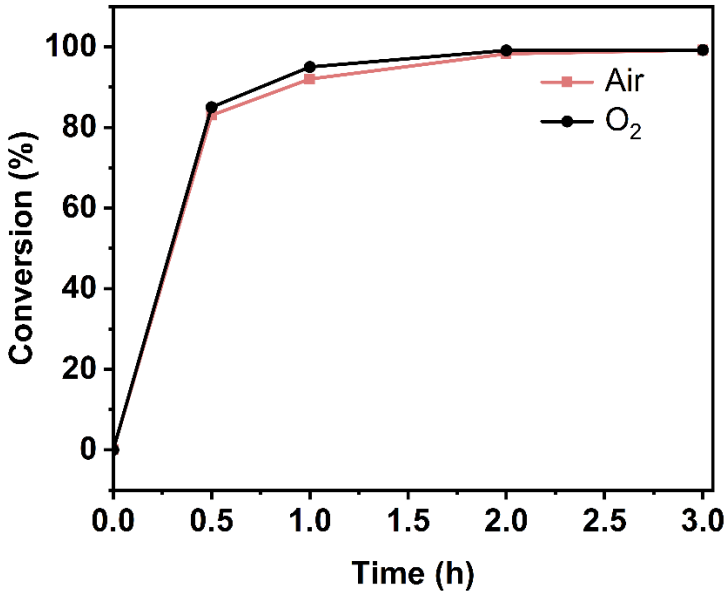

Fig. S10. COF-OMe photocatalyst for selective photocatalytic detoxification of CEES in air and oxygen environments. Standard conditions: COFs (5 mg), CH_3OH (5 mL), CEES (0.2 mmol), white LED. Reaction time: 3h.

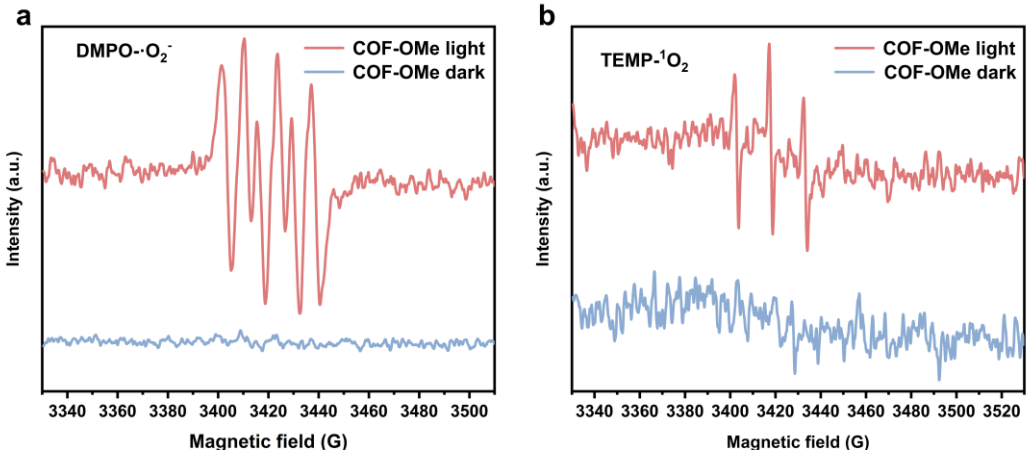

Fig. S11. EPR spectra obtained over COF-OMe under white LEDs irradiation and dark condition.

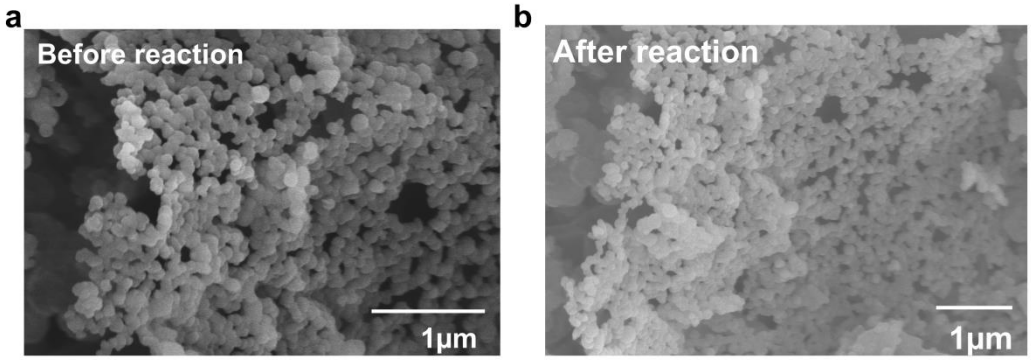

Fig. S12. SEM spectra of COF-OMe before and after reaction.

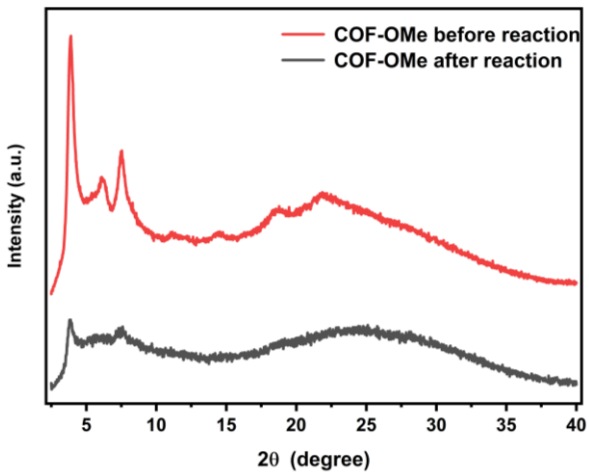

Fig. S13. PXRD characterization of COF-OMe before and after reaction.

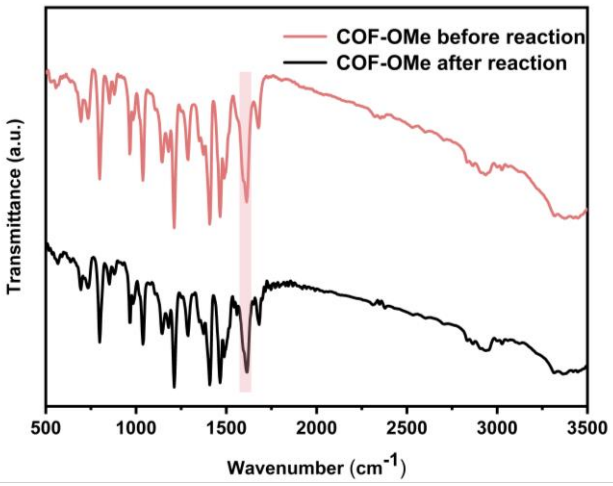

Fig. S14. FT-IR spectra of COF-OMe before and after reaction.

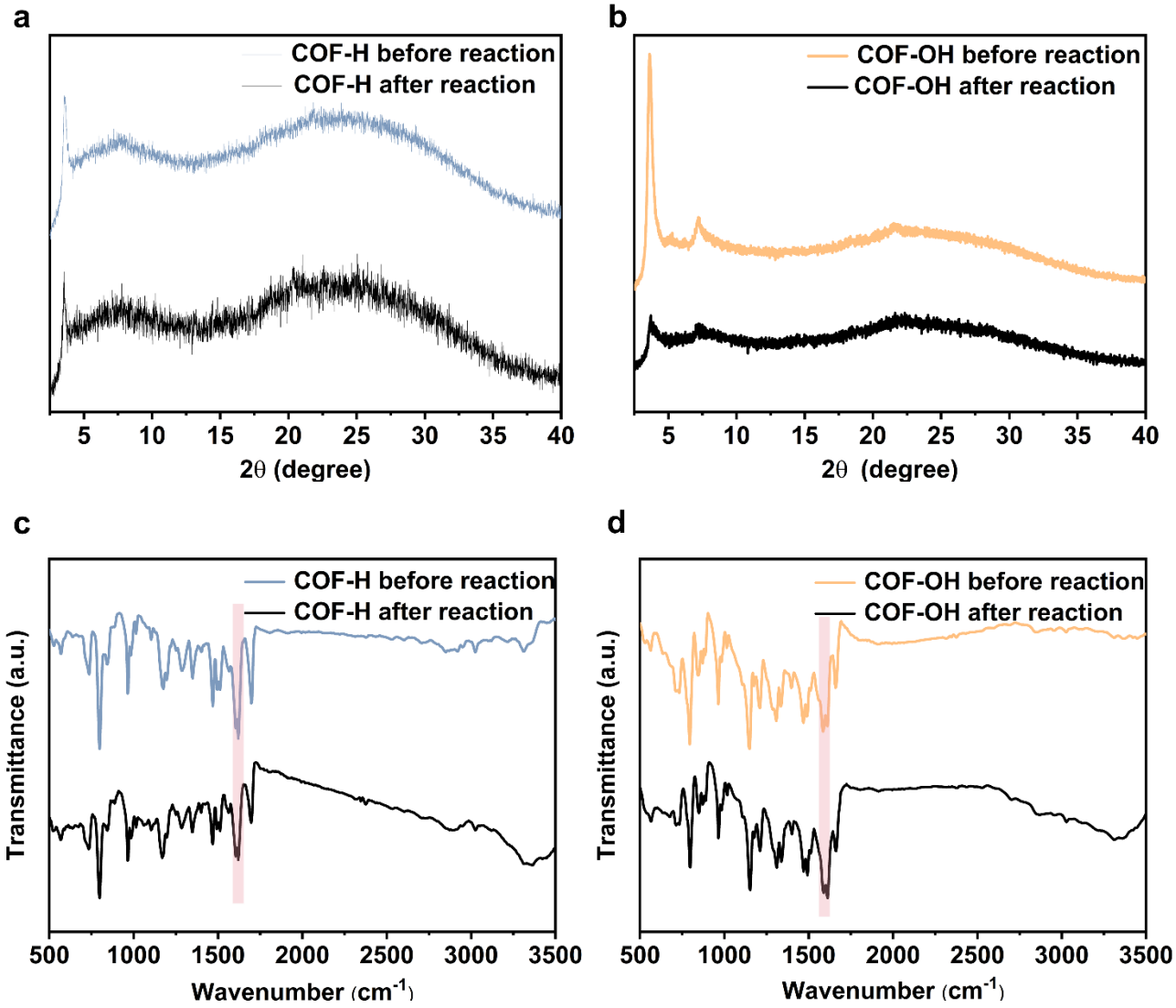

Fig. S15. PXRD characterization COF-H (a) and COF-OH (b); FT-IR spectra of COF-H (c) and COF-OH (d) before and after reaction.

Table S1. The BET surface areas and pore size of COF-H, COF-OH and COF-OMe.

COFs materials	The BET surface areas (m^2/g)	Pore size (nm)
COF-H	211.4	1.91
COF-OH	515.8	1.96
COF-OMe	592.3	1.87

Table S2. Performance of CEES photocatalytic oxidation using various porous materials.

Photocatalysts	Solvent	Atmosphere	light	Conversion	Ref.
NU-400	methanol	O_2	Ultraviolet light	$t_{1/2}$=10.2 min	1
NU-1000	methanol	O_2	Ultraviolet light	$t_{1/2}$=6.2 min	2
In_2S_3/NU-1000	methanol	O_2	Simulated sunlight	3h, 90%	3
NU-1000-PCBA	methanol	O_2	UV (450nm)	t1/2 = 3.5 min	4
Br-BDP@NU-1000	methanol	O_2	green light (325nm)	t1/2 = 2.5 min	5
Ag_{12}TpyP	Ethanol	O_2	White light (80nm)	t1/2 = 1.5 min	6
PCN-222	Methanol	O_2	Blue light	$t_{1/2}$=13min	7
TBP⊂ExBox•PSS	methanol	O_2	UV (500nm)	t1/2 =5min	8
I-BDP-POP	MeOH	O_2	green LED (450nm)	t1/2 =3min	9
Fe-TCPP-La	Methanol	O_2	blue LED	t1/2 =2.5min	10
CzBSe-CMP	methanol	O_2	Blue LED lamp (30 W, 460 nm)	1h, 99%	11
MOF/BA/textile	No solvent	Air	Simulated sunlight	$t_{1/2}$=17.6 min	12
Ag@TAPP-TFPT	Methanol	O_2	Xe light	t1/2 =6.5 min	13
TiO_2/PMA SNBs	methanol	Air	xenon lamp	20min, 98.29%	14
PCN-224@TiO_2	DMF	Air	Simulated sunlight	$t_{1/2}$=330 min	15
COF-OMe	Methanol	Air	white LED	2h,99%	this work

Table S3. The material cost and operation cost of different COFs for CEES photocatalytic oxidation.

Materials	Material Cost ($ /g)	Operation Cost ($ /g)	Ref
BTT-TPh-O-COF	228.2	CD_3OD (5g/64.4), O_2(1atm/0.424)	[16]
Por-Aminal-COF	698.8	CD_3OD (5g/64.4), O_2(1atm/0.424)	[17]
PW12-Ag@COF	97.9	CD_3OD (5g/64.4), O_2(1atm/0.424)	[18]
Ag@TAPP−TFPT	127.2	CD_3OD (5g/64.4), O_2(1atm/0.424)	[13]
COF-H	39.1	Methanol (5g/0.07) Air (0)	this work
COF-OH	58.2	Methanol (5g/0.07) Air (0)	this work
COF-OMe	53.8	Methanol (5g/0.07) Air (0)	this work

References

1. G. Ayoub, M. Arhangelskis, X. Zhang, F. Son, T. Islamoglu, T. Friščić and O. K. Farha, *Beilstein Journal of Nanotechnology*, 2019, **10**, 2422-2427.
2. Y. Liu, C. T. Buru, A. J. Howarth, J. J. Mahle, J. H. Buchanan, J. B. DeCoste, J. T. Hupp and O. K. Farha, *Journal of Materials Chemistry A*, 2016, **4**, 13809-13813.
3. L. Wang, D. Shen, H. Zhang, B. Mo, J. Wu and H. Hou, *Chemistry–A European Journal*, 2022, **28**, e202103466.
4. A. J. Howarth, C. T. Buru, Y. Liu, A. M. Ploskonka, K. J. Hartlieb, M. McEntee, J. J. Mahle, J. H. Buchanan, E. M. Durke and S. S. Al-Juaid, *Chemistry–A European Journal*, 2017, **23**, 214-218.
5. A. Atilgan, T. Islamoglu, A. J. Howarth, J. T. Hupp and O. K. Farha, *ACS applied materials & interfaces*, 2017, **9**, 24555-24560.
6. M. Cao, R. Pang, Q.-Y. Wang, Z. Han, Z.-Y. Wang, X.-Y. Dong, S.-F. Li, S.-Q. Zang and T. C. Mak, *Journal of the American Chemical Society*, 2019, **141**, 14505-14509.
7. Y. Liu, A. J. Howarth, J. T. Hupp and O. K. Farha, *Angewandte Chemie*, 2015, **127**, 9129-9133.
8. Y. Beldjoudi, A. Atilgan, J. A. Weber, I. Roy, R. M. Young, J. Yu, P. Deria, A. E. Enciso, M. R. Wasielewski and J. T. Hupp, *Advanced Materials*, 2020, **32**, 2001592.
9. A. Atilgan, M. M. Cetin, J. Yu, Y. Beldjoudi, J. Liu, C. L. Stern, F. M. Cetin, T. Islamoglu, O. K. Farha and P. Deria, *Journal of the American Chemical Society*, 2020, **142**, 18554-18564.
10. Z.-H. Long, D. Luo, K. Wu, Z.-Y. Chen, M.-M. Wu, X.-P. Zhou and D. Li, *ACS Applied Materials & Interfaces*, 2021, **13**, 37102-37110.
11. Y. Zhi, Z. Yao, W. Jiang, H. Xia, Z. Shi, Y. Mu and X. Liu, *ACS applied materials & interfaces*, 2019, **11**, 37578-37585.
12. Y. Hao, E. K. Papazyan, Y. Ba and Y. Liu, *ACS Catalysis*, 2021, **12**, 363-371.
13. L. Zhang, C. Sun, S.-J. Xiao, Q.-G. Tan, G.-P. Yang, J.-Q. Fan, Y.-T. Luo, R.-P. Liang and J.-D. Qiu, *ACS Applied Nano Materials*, 2023, **6**, 17083-17091.
14. Y. T. Wang, G. H. Chen, Q. Wang, H. Zang, Q. Wang, Y. F. Li, H. Y. Zou, L. Zhan, J. W. Xie and C. Z. Huang, *Small*, 2024, 2407980.
15. X. Hu, Y. Yang, N. Li, C. Huang, Y. Zhou, L. Zhang, Y. Zhong, Y. Liu and Y. Wang, *Journal of Colloid and Interface Science*, 2024, **674**, 791-804.
16. S. Li, L. Dai, L. Li, A. Dong, J. Li, X. Meng, B. Wang and P. Li, *Journal of Materials Chemistry A*, 2022, **10**, 13325-13332.
17. Q. Y. Wang, J. Liu, M. Cao, J. H. Hu, R. Pang, S. Wang, M. Asad, Y. L. Wei and S. Q. Zang, *Angewandte Chemie*, 2022, **134**, e202207130.
18. Q. Zhu, H. An, T. Xu, S. Chang, Y. Chen, H. Luo and Y. Huang, *Applied Catalysis A: General*, 2023, **662**, 119283.